Xin Tong,[1] Tatsuyoshi Kono,[2] Emily K. Anderson-Baucum,[2] Wataru Yamamoto,[1] Patrick Gilon,[3] Djamel Lebeche,[4] Richard N. Day,[1] Gary E. Shull,[5] and Carmella Evans-Molina[1,2,6,7,8]

SERCA2 Deficiency Impairs Pancreatic β-Cell Function in Response to Diet-Induced Obesity

Diabetes 2016;65:3039–3052 | DOI: 10.2337/db16-0084

The sarcoendoplasmic reticulum (ER) Ca^{2+} ATPase 2 (SERCA2) pump is a P-type ATPase tasked with the maintenance of ER Ca^{2+} stores. Whereas β-cell SERCA2 expression is reduced in diabetes, the role of SERCA2 in the regulation of whole-body glucose homeostasis has remained uncharacterized. To this end, SERCA2 heterozygous mice (S2HET) were challenged with a high-fat diet (HFD) containing 45% of kilocalories from fat. After 16 weeks of the HFD, S2HET mice were hyperglycemic and glucose intolerant, but adiposity and insulin sensitivity were not different between HFD-fed S2HET mice and HFD-fed wild-type controls. Consistent with a defect in β-cell function, insulin secretion, glucose-induced cytosolic Ca^{2+} mobilization, and the onset of steady-state glucose-induced Ca^{2+} oscillations were impaired in HFD-fed S2HET islets. Moreover, HFD-fed S2HET mice exhibited reduced β-cell mass and proliferation, altered insulin production and proinsulin processing, and increased islet ER stress and death. In contrast, SERCA2 activation with a small molecule allosteric activator increased ER Ca^{2+} storage and rescued tunicamycin-induced β-cell death. In aggregate, these data suggest a critical role for SERCA2 and the regulation of ER Ca^{2+} homeostasis in the β-cell compensatory response to diet-induced obesity.

Type 2 diabetes (T2D) is a metabolic disorder affecting more than 415 million individuals worldwide that is characterized by peripheral insulin resistance and inadequate insulin secretion from the pancreatic β-cell (1). During the development of T2D and in the face of advancing peripheral insulin resistance, the β-cell undergoes a functional and proliferative compensatory response to increase insulin output and maintain euglycemia. The ability of the β-cell to continue in this extended state of compensation is finite for a substantial proportion of individuals, and the typical evolution to T2D is characterized by loss of pancreatic β-cell function, mass, and, possibly, identity (2,3).

As a secretory endocrine cell, the β-cell relies on a highly developed and active endoplasmic reticulum (ER) to ensure that insulin is robustly produced and efficiently folded. Notably, the ER also serves as a dominant intracellular store of Ca^{2+}, and the intraluminal ER Ca^{2+} concentration is estimated to be ~30–300 μmol/L, an amount at least three orders of magnitude higher than cytosolic Ca^{2+} (4,5). The integrity of this transmembrane Ca^{2+} gradient is maintained largely through activity of the sarco-ER Ca^{2+} ATPase 2b (SERCA2b) pump that actively transports two Ca^{2+} ions into the ER lumen during each catalytic cycle (6). Within the ER, Ca^{2+} serves as a critical cofactor for protein chaperones and foldases, whereas β-cell insulin secretion is patterned by a dynamic cross talk between the ER and cytosolic Ca^{2+} pools (7–9).

To date, at least 14 different SERCA isoforms have been identified in mammals (10). We previously showed

[1]Department of Cellular and Integrative Physiology, Indiana University School of Medicine, Indianapolis, IN
[2]Department of Medicine, Indiana University School of Medicine, Indianapolis, IN
[3]Pôle d'endocrinologie, diabète et nutrition, Institut de recherche expérimentale et clinique, Université catholique de Louvain, Brussels, Belgium
[4]Cardiovascular Research Institute and Diabetes Obesity and Metabolism Institute, Department of Medicine, Icahn School of Medicine at Mount Sinai, New York, NY
[5]Department of Molecular Genetics, Biochemistry, and Microbiology, University of Cincinnati College of Medicine, Cincinnati, OH
[6]Department of Biochemistry and Molecular Biology, Indiana University School of Medicine, Indianapolis, IN
[7]Herman B Wells Center for Pediatric Research, Indiana University School of Medicine, Indianapolis, IN
[8]Roudebush VA Medical Center, Indianapolis, IN
Corresponding author: Carmella Evans-Molina, cevansmo@iu.edu.

Received 17 January 2016 and accepted 28 July 2016.
This article contains Supplementary Data online at http://diabetes.diabetesjournals.org/lookup/suppl/doi:10.2337/db16-0084/-/DC1.

SERCA2b is the most prevalent isoform expressed in the pancreatic islet (11). Moreover, we and others have demonstrated significantly reduced islet SERCA2b expression and activity under diabetic and inflammatory conditions (11–14). However, the role of SERCA2 in the regulation of whole-body glucose homeostasis remains largely uncharacterized. To this end, mice with whole-body SERCA2 heterozygous deficiency (S2HET) were challenged with a high-fat diet (HFD), and metabolic analysis was performed. Here, we show that SERCA2 deficiency, which occurs in human Darier-White disease (15), leads to glucose intolerance, decreased insulin secretion, reduced β-cell proliferation, and increased β-cell ER stress. Together, these data suggest a critical role for SERCA2 activity and the maintenance of β-cell ER Ca^{2+} homeostasis in the compensatory response to diet-induced obesity and raise the possibility that individuals with Darier-White disease may have an increased susceptibility to metabolic disease.

RESEARCH DESIGN AND METHODS

Animal, Islet, and Cell-Based Studies

S2HET mice were developed by Gary E. Shull (University of Cincinnati), backcrossed onto a C57BL6/J background for at least 10 generations, and maintained under protocols approved by the Indiana University Institutional Animal Care and Use Committee. Male S2HET mice and wild-type (WT) littermate controls were fed an HFD containing 45% of kilocalories from fat (Harlan Laboratories, Indianapolis, IN) beginning at 8 weeks of age. Intraperitoneal glucose tolerance tests (IPGTT) and oral glucose tolerance tests (OGTT) were performed after 6 h of fasting and administration of glucose at a dose of 2 g/kg total body weight. Insulin tolerance tests were performed after a 5- to 6-h fast and administration of regular human insulin at a dose of 0.75 IU/kg of total body weight. To assess insulin signaling, mice were fasted for 6 h and injected intraperitoneally with insulin (10 IU/kg of total body weight) or saline. After 10 min, liver, epididymal adipose, and gastrocnemius skeletal muscle tissue were harvested for immunoblot. Glucose levels were measured using the AlphaTRAK glucometer (Abbott Laboratories, Abbott Park, IL). Serum insulin and proinsulin levels were measured using ELISAs from Crystal Chem (Chicago, IL) and ALPCO Diagnostics (Salem, NH), respectively. DEXA analysis was performed to estimate body composition using the Lunar PIXImus II (GE Medical Systems) mouse DEXA. To assess β-cell death, droplet digital PCR was used to measure serum levels of unmethylated insulin DNA using a QX200 Droplet Digital PCR System from Bio-Rad Laboratories, as previously described (16).

β-Cell mass and proliferation were assessed as detailed previously (17) using the antibodies outlined in Supplementary Table 1. Mouse pancreatic islets were isolated by collagenase digestion as previously described (18). Isolated islets were fixed in 2% glutaraldehyde and 4% paraformaldehyde in 0.1 mol/L sodium cacodylate buffer and transferred to the Advanced Electron Microscopy Facility at the University of Chicago to generate transmission electron micrographic images. The relative percentages of mature, immature, and rod-like secretory granules were quantitated manually using ImageJ software, as previously described (19).

A clustered regularly interspaced short palindromic repeats (CRISPR)/Cas 9 technique was used to produce an SERCA2 knockout (KO) INS-1 832/13 cell line in the Genome Engineering Center (GEC) at Washington University in St. Louis (St. Louis, MO). For SERCA2b rescue studies, KO and parent INS-1 cells were transduced with an adenovirus expressing SERCA2b or LacZ (12). INS-1 cells or mouse islets were cultured in RPMI containing 25 mmol/L glucose and 500 μmol/L BSA-conjugated palmitate for 24 h to mimic the diabetic milieu (20). The Promega CellTiter-Glo Luminescent Cell Viability Assay (Madison, WI) was used according to the manufacturer's instructions.

Glucose-stimulated insulin secretion (GSIS), immunoblot, and immunofluorescence in cultured INS-1 cells and isolated mouse islets were performed as previously described (11,12). Quantitative real-time PCR was performed using previously published primer sequences (11) or the primers outlined in Supplementary Table 2. CDN1163 was a gift from Djamel Lebeche (Icahn School of Medicine at Mount Sinai).

Cytosolic and ER Ca^{2+} Imaging

Cytosolic Ca^{2+} dynamics in INS-1 cells were assessed using the FLIPR Calcium 6 Assay Kit (Molecular Devices, Sunnyvale, CA), as previously described (13). The ratiometric Ca^{2+} indicator fura-2-acetoxymethylester (Fura-2 AM) (Life Technologies) was used for islet cytosolic Ca^{2+} imaging experiments using a Zeiss Z1 microscope, as previously published (21). To directly image ER Ca^{2+} in individual β-cells, mouse islets were dispersed with Accutase (Innovative Cell Technologies, Inc., San Diego, CA), and 10^5 dispersed islets cells were seeded in imaging dishes pretreated with poly-L-lysine (Sigma-Aldrich, St. Louis, MO). Dispersed islets and INS-1 cells were transduced with the ER-directed Ca^{2+} biosensor D4ER adenovirus, and fluorescence lifetime imaging microscopy (FLIM) was used to monitor ER Ca^{2+} levels in accordance with previously published protocols (12).

Statistical Analysis

Differences between groups were analyzed for significance using the unpaired Student *t* test or one-way ANOVA with Tukey-Kramer post hoc analysis. Results are reported as the means ± SEM. GraphPad Prism software (GraphPad Software, Inc., La Jolla, CA) was used for data analysis. A P value < 0.05 was taken to indicate the presence of a significant difference between groups.

RESULTS

Whole-Body SERCA2 Haploinsufficiency Leads to Impaired Glucose Tolerance in Response to Diet-Induced Obesity

To define the role of SERCA2 in the compensatory response to diet-induced obesity, S2HET and WT mice were challenged with an HFD containing 45% of kilocalories from fat beginning at 8 weeks of age. Islet SERCA2 levels were suppressed by the expected 50% before (PreHFD) and after the HFD, and no changes in SERCA3 protein or mRNA

expression were observed (Fig. 1*A–C*). Moreover, the percentage of lean and fat mass was identical between groups PreHFD and after HFD, and temporal patterns of weight gain in response to HFD were no different between genotypes (Fig. 1*D* and *E*). In contrast, after HFD, S2HET mice demonstrated significantly higher fasting blood glucose levels and lower fed insulin levels compared with HFD-fed WT controls (Fig. 1*F* and *G*).

WT and S2HET mice were challenged with intraperitoneal or oral glucose (IPGTT and OGTT) before and/or after 16 weeks of the HFD. Although no differences in glucose tolerance were observed at baseline between PreHFD-S2HET and WT mice, glucose tolerance in both groups was significantly worsened by the HFD. Furthermore, in response to both the intraperitoneal and oral glucose challenge, HFD-fed S2HET mice exhibited significantly increased glucose excursions and reduced glucose tolerance compared with HFD-fed WT controls, as assessed by area under the curve analysis (Fig. 1*H–K*).

Although insulin tolerance tests revealed significantly decreased insulin sensitivity after the HFD in both S2HET and WT mice, no differences were observed between genotypes (Fig. 2*A* and *B*). Next, levels of AKT phosphorylation at serine 473 in the epididymal adipose tissue, liver, and gastrocnemius skeletal muscle were measured after acute insulin or saline administration. Again, no differences were observed between HFD-fed S2HET and WT mice (Fig. 2*C–E*).

SERCA2 Deficiency Results in Impaired GSIS

Initial analysis of HFD-fed S2HET mice revealed hyperglycemia, reduced serum insulin levels, and impaired glucose tolerance without apparent alterations in insulin sensitivity or adiposity, suggesting a primary defect in β-cell function. To define further the β-cell phenotype associated with in vivo SERCA2 deficiency, insulin levels were measured in HFD-fed S2HET and WT controls after a 5-h fast and 10 min after an intraperitoneal glucose injection. In response to the glucose challenge, serum insulin levels were significantly lower in the HFD-fed S2HET mice than in the HFD-fed WT controls (Fig. 3*A*). Similar to in vivo findings, results from ex vivo GSIS assays revealed a significant decrease in insulin secretion in islets isolated from HFD-fed S2HET mice (Fig. 3*B*).

SERCA2 Deficiency Leads to Impaired Islet Ca^{2+} Homeostasis

Next, Ca^{2+} imaging experiments using Fura-2 AM were performed in islets isolated from PreHFD and HFD-fed WT and S2HET mice. PreHFD, no differences in baseline cytosolic Ca^{2+} levels were observed between S2HET and WT islets. However, baseline cytosolic Ca^{2+} levels were increased by the HFD in both genotypes, with S2HET islets exhibiting a significantly larger increase in baseline cytosolic Ca^{2+} (Fig. 4*A–C*). The HFD also induced a significant delay in the onset of steady-state cytosolic Ca^{2+} oscillations in response to glucose (phase 1 duration) in both WT and S2HET islets. Again, compared with PreHFD-S2HET and WT islets and HFD-fed WT islets, HFD-S2HET islets exhibited a significantly longer phase 1 duration (Fig. 4*D*). The HFD similarly increased the initial glucose-stimulated Ca^{2+} response (phase 1 amplitude; ΔF1) in WT islets. However, the phase 1 amplitude was blunted in HFD-S2HET islets compared with islets from HFD-fed WT controls (Fig. 4*E*). The amplitude of the oscillatory response (relative oscillatory amplitude; ΔF2) was not significantly different between groups (Fig. 4*F*). To assess the response to another secretagogue, islets from HFD-fed WT and S2HET mice were treated with 30 mmol/L KCl. Similar to the ΔF1 response to glucose, Ca^{2+} mobilization in response to KCl was also decreased in islets isolated from HFD-S2HET mice (Fig. 4*G* and *H*).

FLIM was next used to monitor directly ER Ca^{2+} levels in dispersed islets from PreHFD-WT and S2HET mice. Dispersed islets were transduced with an adenovirus encoding the D4ER Ca^{2+} biosensor probe (9) and then treated for 48 h with or without 25 mmol/L glucose and 500 μmol/L BSA-conjugated palmitate (control or glucolipotoxicity [GLT]) to mimic in vivo HFD conditions. FLIM was used to monitor the change in donor lifetime that results from Ca^{2+} binding to the biosensor. Analysis revealed lower ER Ca^{2+} levels in S2HET β-cells, as indicated by the reduced change in the donor lifetime of the biosensor, and this was further exacerbated by GLT (Fig. 4*I* and *J*).

SERCA2 Deficiency Results in Altered Insulin Production, Processing, and Packaging

To test whether changes in β-cell calcium homeostasis were sufficient to affect insulin biosynthesis, total insulin content and insulin mRNA levels were measured in isolated islets, and both were found to be significantly reduced in HFD-fed S2HET mice compared with HFD-fed WT controls (Fig. 5*A* and *B*). Furthermore, compared with HFD-fed WT controls, HFD-fed S2HET mice exhibited a nearly threefold increase in the serum proinsulin-to-insulin ratio (Fig. 5*C*), suggesting a parallel decrease in proinsulin maturation.

Insulin granule morphology was next assessed by quantitative analysis of islet electron micrographic images. Typical mature insulin granules were defined according to previously published protocols (22) and exhibited a dense homogenous core with a clear halo, whereas immature granules exhibited an empty or lighter core and the absence of a defined halo (Fig. 5*D*) (19). The percentage of immature granules was nearly twofold higher in HFD-fed S2HET mice than in HFD-fed WT controls. In addition, HFD-S2HET islets displayed a significantly higher percentage of rod-like granules, indicating defective insulin crystallization and packaging (Fig. 5*E*). Consistent with observed defects in insulin processing, proprotein convertase (PC) 1/3 mRNA levels were significantly decreased in islets isolated from HFD-fed S2HET mice, and there was a trend toward reduced PC1/3 protein expression (Fig. 5*F–H*).

SERCA2 Haploinsufficient Mice Exhibit Reduced β-Cell Proliferation and β-Cell Mass and Increased β-Cell Death in Response to the HFD

β-Cell mass was quantitated before and after 16 weeks of the HFD. There was no significant difference in β-cell

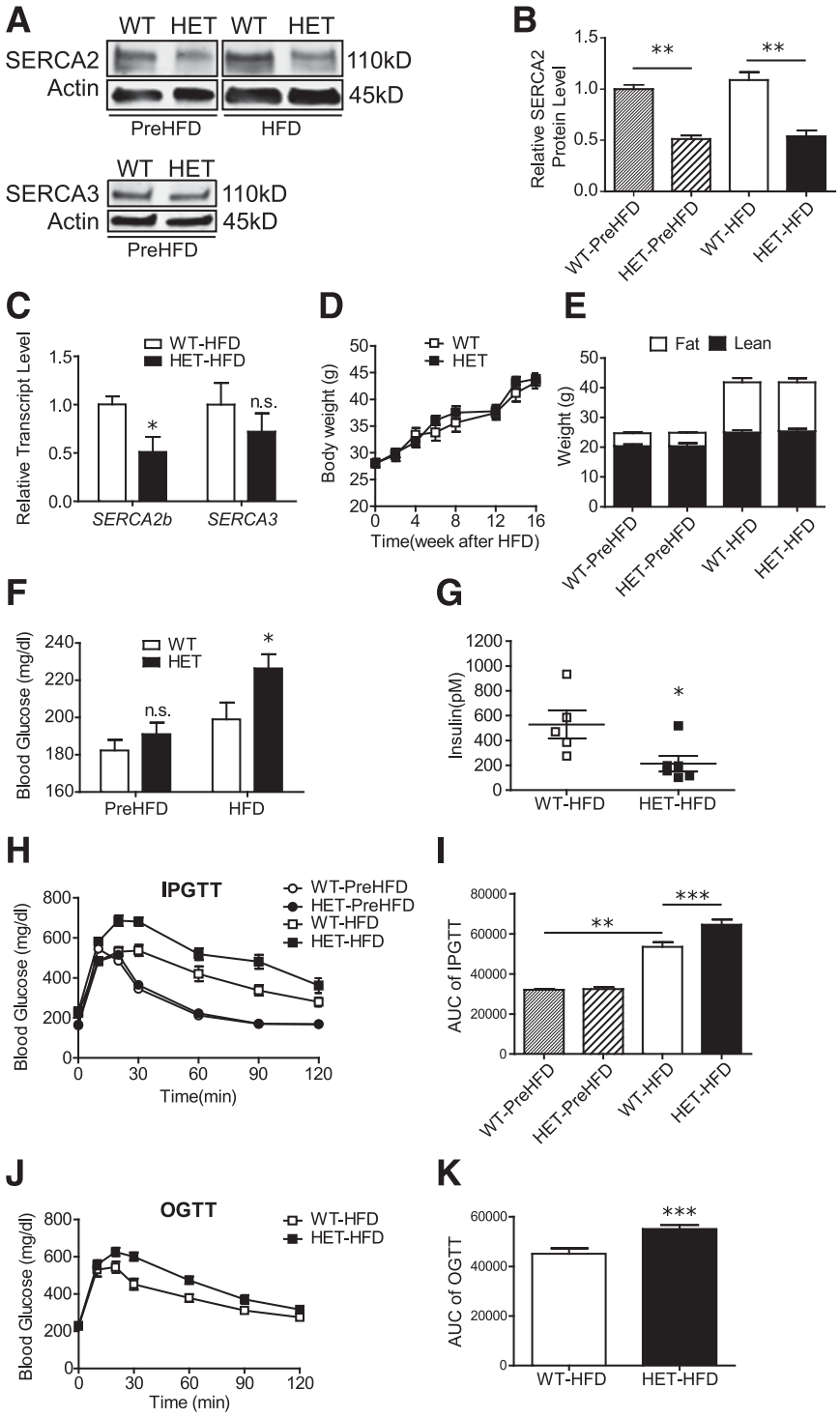

Figure 1—S2HET mice exhibit impaired glucose tolerance in response to HFD. SERCA2 HET and WT littermate controls were fed an HFD containing 45% of kilocalories from fat for 16 weeks starting at 8 weeks of age. *A–C*: Protein and RNA were isolated from HET and WT islets before (WT-PreHFD and HET-PreHFD) and after 16 weeks of HFD (WT-HFD and HET-HFD). *A*: Immunoblot analysis was performed using antibodies against SERCA2, SERCA3, and actin. *B*: Quantitative SERCA2 protein levels are shown graphically. *C*: Reverse-transcribed RNA was subjected to real-time quantitative PCR to measure *SERCA2b* and *SERCA3* transcript levels (normalized to *Actb*). *D* and *E*: Longitudinal changes in body weight were measured, and DEXA analysis was performed in HET and WT mice at the start and after 16 weeks of the HFD. *F*: Blood glucose in 6-h fasted WT and HET mice before and after 16 weeks of HFD. *G*: Random-fed serum insulin levels after 16 weeks of the HFD. *H–K*: IPGTT or OGTT were performed before or after 16 weeks of HFD treatment in HET and WT mice; area under the curve (AUC) analysis is shown graphically. Results are displayed as means ± SEM (n = at least 8 per group, except panel *F*, where n = 19 for S2HET group, and *G*, where n is indicated by the scatterplot). Indicated comparisons are significantly different: *$P < 0.05$; **$P < 0.01$; ***$P < 0.001$; n.s. indicates that no significant differences were observed between groups.

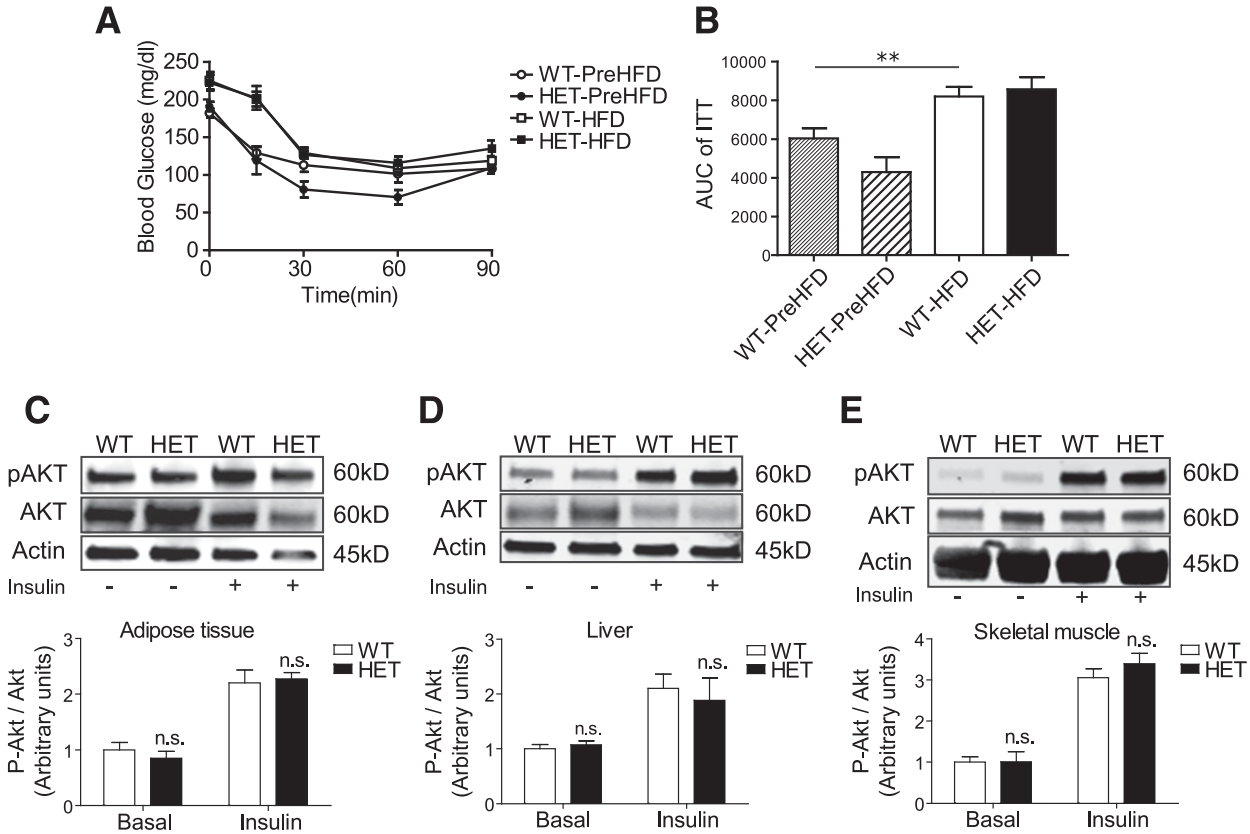

Figure 2—HFD-fed S2HET and WT mice exhibit comparable levels of insulin sensitivity. *A* and *B*: Insulin tolerance tests were performed before (WT-PreHFD and HET-PreHFD) and after 14 weeks of HFD feeding (WT-HFD and HET-HFD), with area under the curve (AUC) analysis shown graphically. Protein homogenates from adipose (*C*), liver (*D*), or skeletal muscle (*E*) were obtained from saline (basal) or insulin-injected HET and WT mice fed the HFD for 16 weeks. Immunoblot analysis was performed using antibodies against phosphorylated (p)AKT (ser473), total AKT, and actin. Relative protein levels are shown graphically. Results are displayed as means ± SEM (n = 6 per group). Indicated comparisons are significantly different: $^{**}P < 0.01$; n.s. indicates that no significant differences were observed between groups.

mass between 8-week-old PreHFD-S2HET and WT control mice. In contrast, HFD-S2HET mice demonstrated significantly lower β-cell mass than age-matched HFD-fed WT controls (Fig. 6*A* and *B*). However, no significant difference in the number of α-cells per islet was noted between genotypes (Fig. 6*C* and *D*). To assess β-cell proliferation, pancreatic sections were stained with antibodies against insulin and proliferating cell nuclear antigen, and double-positive cells were counted. Results indicated a significant reduction in the percentage of proliferating β-cells in the

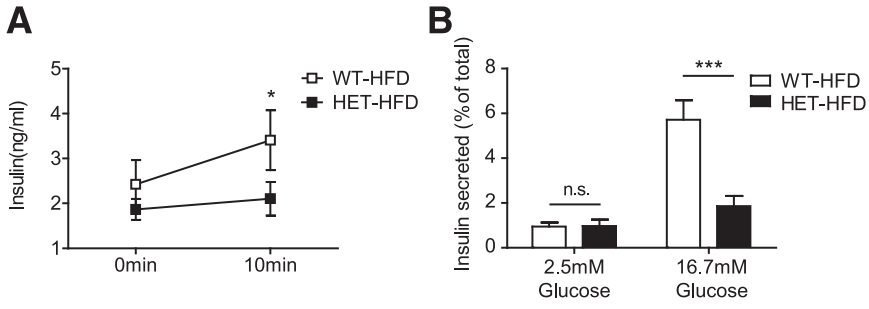

Figure 3—SERCA2 deficiency leads to decreased insulin secretion. *A*: Serum insulin levels were measured in S2HET (HET) and WT mice fed the HFD for 16 weeks at time 0 after a 5-h fast and 10 min after an intraperitoneal injection of glucose (2 mg/kg total body weight). *B*: Islets were isolated from HFD-fed S2HET and WT mice, and GSIS was measured and normalized to total insulin content. Results are displayed as the means ± SEM from three or more independent experiments for each group. Indicated comparisons are significantly different: $^{*}P < 0.05$; $^{***}P < 0.001$; n.s. indicates that no significant differences were observed between groups.

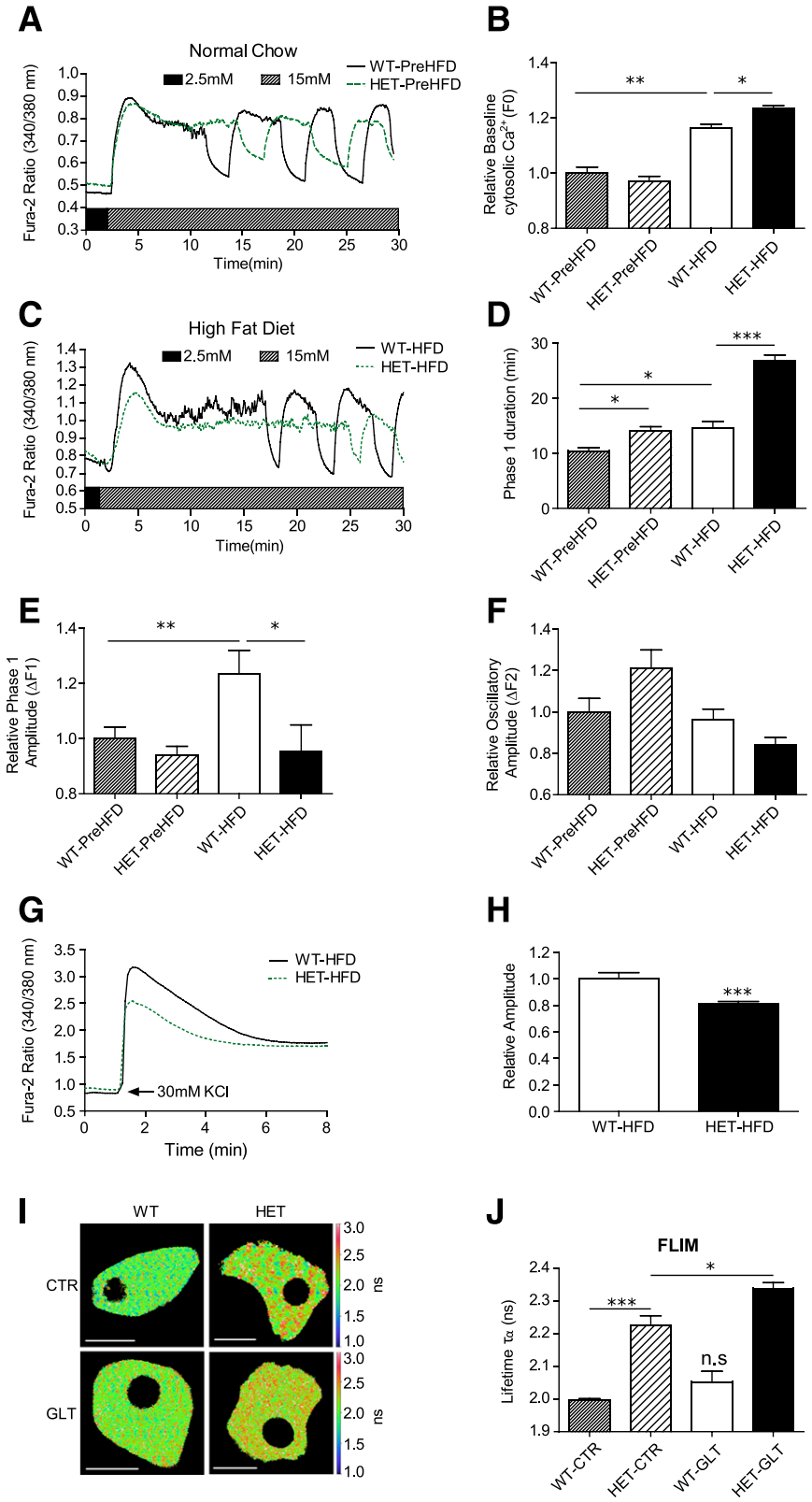

Figure 4— Islets isolated from S2HET mice exhibit impaired Ca^{2+} homeostasis. Islets were isolated from 8-week-old PreHFD-WT mice or WT mice fed the HFD for 16 weeks and 8-week-old PreHFD-S2HET mice or S2HET mice fed the HFD for 16 weeks. Isolated islets were loaded with Fura-2 AM, and Ca^{2+} imaging was performed. *A* and *C*: Representative cytosolic Ca^{2+} recording of islets after stimulation with 15 mmol/L glucose. *B*: Quantification of the relative basal cytosolic Ca^{2+} (F0) in WT and HET islets. *D*: Quantification of the phase 1 duration. *E*: Quantification of the phase 1 cytosolic Ca^{2+} amplitude. *F*: Quantification of the average cytosolic Ca^{2+} oscillatory amplitude from five continuous oscillatory cycles per islet. *G*: Representative cytosolic Ca^{2+} recording from WT-HFD and HET-HFD islets after stimulation with 30 mmol/L KCl. *H*: Quantification of the phase 1 cytosolic Ca^{2+} amplitude in response to KCl (*n* = at least 26 islets from 3 biological replicates per group for *A*–*H*).

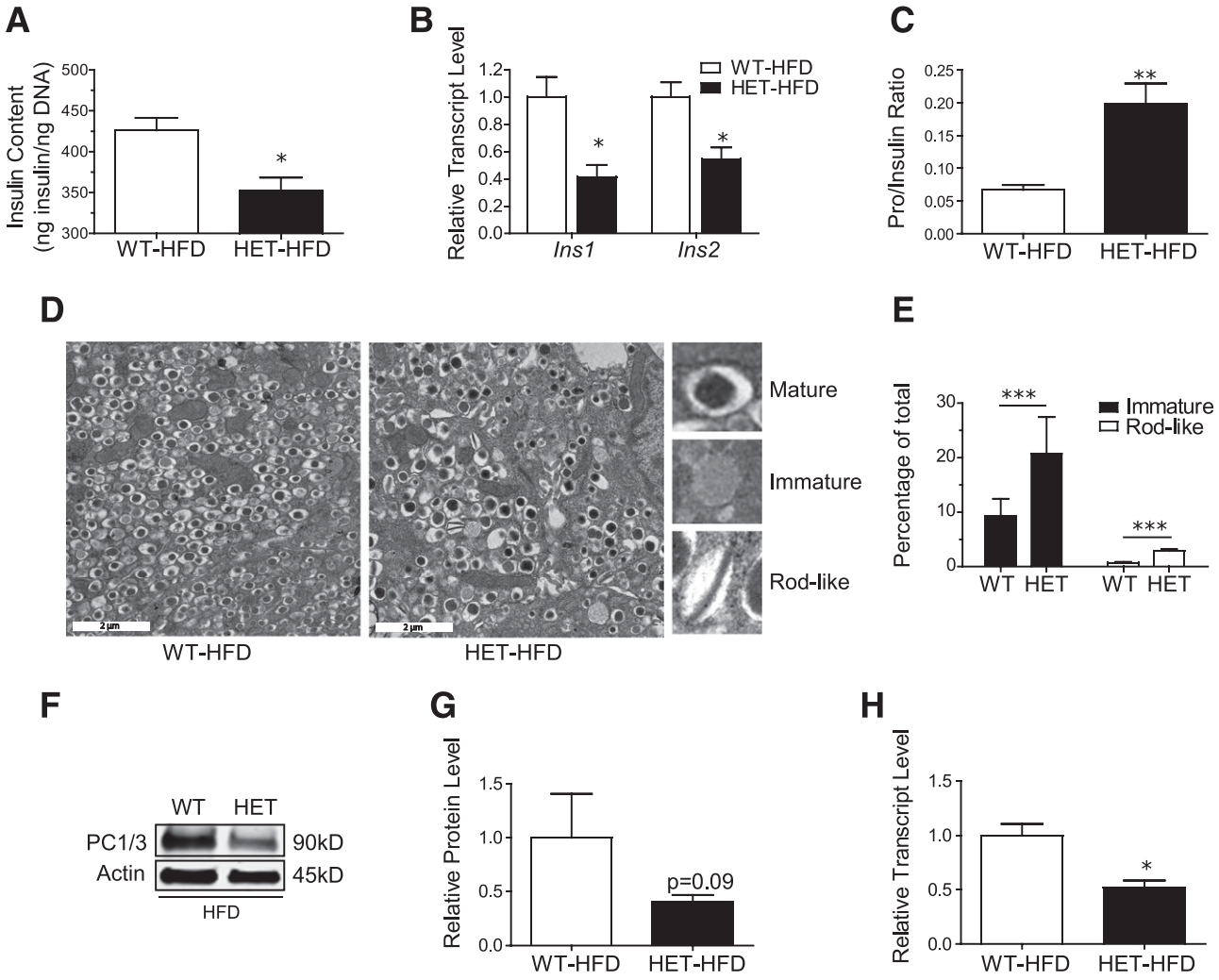

Figure 5—HFD-fed S2HET mice exhibit impaired insulin production, processing, and granule maturation. Islets were isolated from HFD-fed S2HET (HET) and WT mice. *A*: Total islet insulin content was normalized to islet DNA content. *B*: *Ins1* and *Ins2* transcript levels were measured by quantitative real-time PCR and normalized to *Actb* levels. *C*: Serum proinsulin levels were measured after 16 weeks of HFD in WT and S2HET mice. Results are expressed as the ratio of serum proinsulin to insulin (n = 5 biological replicates). *D* and *E*: Islets from WT or S2HET mice (n = 3 each) before and after 16 weeks of HFD were pooled and analyzed by electron microscopy. Representative electron microscopic images of β-cells and insulin granule morphology from HFD-fed WT and HET mice are shown. Panel *E* shows quantitative analysis of 20 images per group (scale bar = 2 μm). *F–H*: Protein and RNA were isolated from HFD-fed WT and HET, and immunoblot analysis was performed using antibodies against PC1/3 and actin. Quantitative PC1/3 protein and transcripts levels are shown graphically. Results are displayed as the means ± SEM. The indicated comparisons are significantly different: $^*P < 0.05$; $^{**}P < 0.01$; $^{***}P < 0.001$.

HFD-fed S2HET mice compared with the HFD-fed WT controls (Fig. 6*E* and *F*). Finally, to assess β-cell death, droplet digital PCR was used to measure circulating levels of unmethylated cell-free *Ins2* DNA (16). PreHFD, S2HET mice exhibited a trend of higher unmethylated DNA levels. After 8 weeks of the HFD, S2HET mice had significantly higher circulating levels of unmethylated *Ins2* DNA. These differences persisted through 12 weeks; however, no differences between groups were noted after 17 weeks of the HFD (Fig. 6*G*).

SERCA2 Deficiency Leads to Activation of β-Cell ER Stress

Our results suggested that SERCA2 haploinsufficiency reduced the ability of the pancreatic islet to compensate for the metabolic challenge of the HFD, resulting in impaired β-cell secretory function, decreased β-cell

I and *J*: Dispersed islets were transduced with a D4ER adenovirus, and FLIM was used to measure ER Ca^{2+}. Representative lifetime map with lookup table indicating donor lifetime in ns (scale bar = 10 μm) and average donor lifetime in PreHFD-WT and S2HET β-cells treated under control (CTR) or GLT conditions (n = at least 10 cells per condition). Results are displayed as means ± SEM. Indicated comparisons are significantly different: $^*P < 0.05$; $^{**}P < 0.01$; $^{***}P < 0.001$; n.s. indicates that no significant differences were observed between groups.

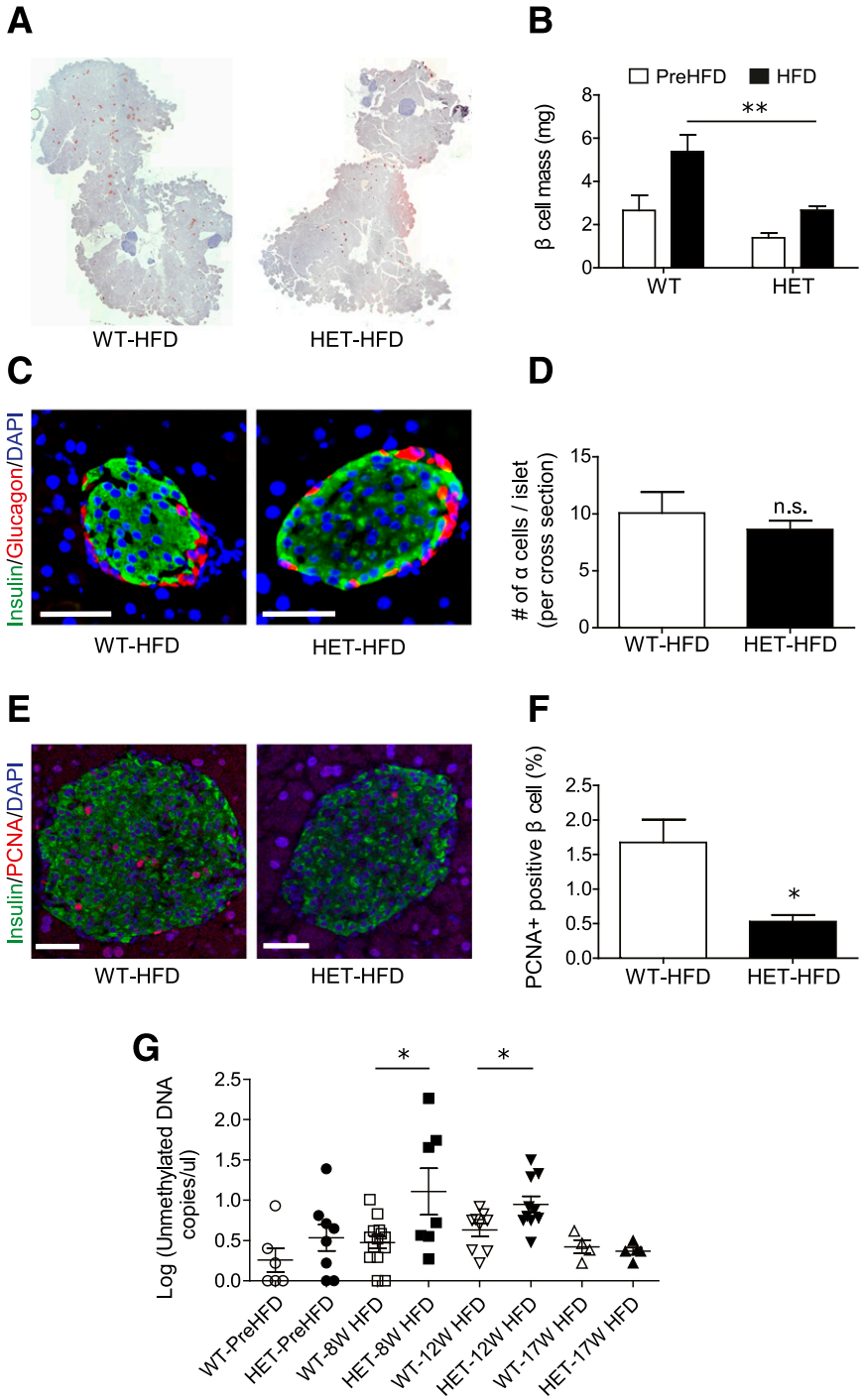

Figure 6—HFD-fed S2HET mice exhibit decreased β-cell mass and proliferation and increased β-cell death. *A*: Representative images of insulin immunohistochemistry in pancreata harvested from HFD-fed S2HET (HET) and WT mice. *B*: β-Cell mass was quantified in WT and HET mice before and after 16 weeks of HFD treatment. *C* and *D*: Representative images of insulin and glucagon immunofluorescence in pancreata harvested from HFD-fed WT and HET mice. Quantification of the number of α-cells per islet is shown graphically. *E* and *F*: Quantification of the percentage of β-cells positive for proliferating cell nuclear antigen (PCNA). *G*: Randomly fed serum was collected from WT and HET mice before and during HFD feeding at indicated time points. Levels of circulating unmethylated mouse *insulin* DNA levels were measured by droplet digital PCR and are depicted as Log (copies/μL). Results are displayed as means ± SEM (*n* = at least 4 biological replicates per group in *A*–*F*, and *n* values are indicated in the scatter plots in panel *G*). Scale bars = 50 μm. The indicated comparisons were significantly different: $^{*}P < 0.05$; $^{**}P < 0.01$; n.s. indicates that no significant differences were observed between groups.

proliferation, and increased β-cell death. To define further the mechanisms underlying these observations, ER morphology was analyzed from electron micrographic images of islets isolated from HFD-fed S2HET and WT mice. In contrast to the regularly spaced stacks of ER sheets observed in β-cells from WT mice, analysis of S2HET β-cells revealed swollen and fragmented ER morphology (Fig. 7*A*). Expression of genes encoding proteins involved in ER stress signaling, including *Dnajc3*, *Hsp90b1*, and *Pdia4*, were significantly increased, and the *spliced Xbp-1*–to–*total Xbp-1* ratio was higher in HFD-S2HET islets (Fig. 7*B*). These findings were confirmed using islets isolated from PreHFD-S2HET and WT control mice that were treated ex vivo with GLT stress. Expression of *Grp78*, *Dnajc3*, *Hsp90b1*, and *Pdia4* were increased at baseline in S2HET islets and further elevated in response to GLT, whereas the *spliced*-to-*total Xbp-1* ratio was significantly increased in GLT-treated S2HET islets compared with levels observed in WT controls (Fig. 7*C*).

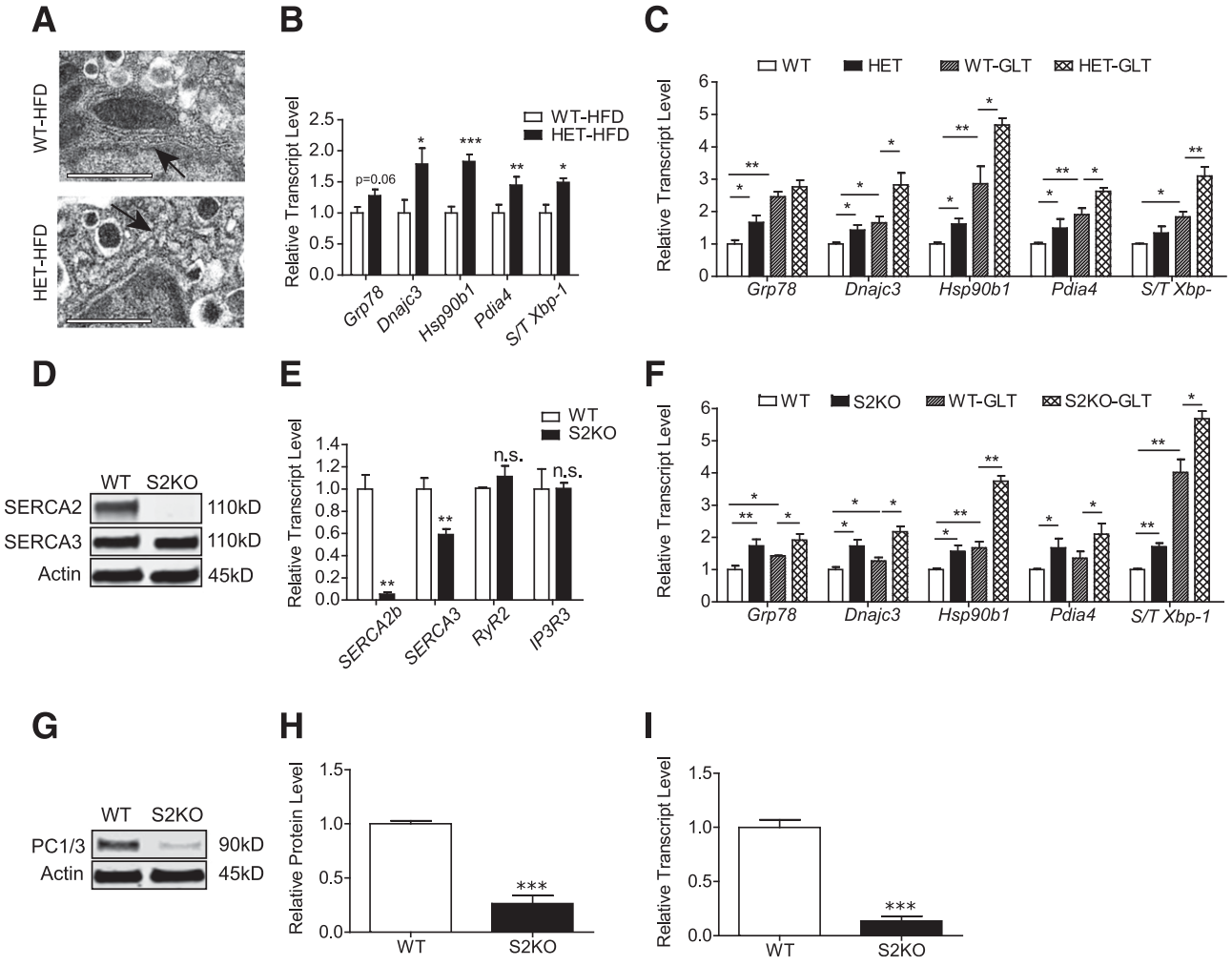

Figure 7—S2HET islets and SERCA2-deficient β-cells exhibit increased ER stress. *A*: Islets from WT or S2HET (HET) mice (n = 3 each) fed the HFD for 16 weeks were pooled, fixed, and analyzed by electron microscopy. Representative images of the β-cell ER structure are shown and indicated by arrows (scale bar = 1 μm). *B*: Islets were isolated from S2HET mice and WT controls fed HFD for 16 weeks (n = 5–6). Reverse-transcribed RNA was subjected to quantitative real-time PCR to measure *Grp78*, *Dnajc3*, *Hsp90b1*, *Pdia4*, *spliced (S)/total (T) Xbp-1*, and *Actb* transcript levels. *C*: Freshly isolated islets from 10-week-old male S2HET and WT mice fed normal chow were treated with or without 25 mmol/L glucose + 500 μmol/L BSA-conjugated palmitate (GLT) for 24 h. Reverse-transcribed RNA was subjected to quantitative real-time PCR to measure indicated gene transcript levels (n = 9 biological replicates analyzed over three individual experiments). *D*: Immunoblot analysis was performed using antibodies against SERCA2, SERCA3, and actin in S2KO INS-1 cells. *E*: Reverse transcribed RNA isolated from S2KO and WT INS-1 cells was subjected to quantitative real-time PCR for quantification of *SERCA2b*, *SERCA3*, *RyR2*, and *IP3R3*, and results were normalized to *Actb* transcript levels. *F*: Reverse-transcribed RNA isolated from S2KO and WT INS-1 cells treated with or without GLT for 24 h was subjected to quantitative real-time PCR for quantification of indicated transcript levels. *G–I*: Protein and RNA were isolated from WT and S2KO INS-1 cells. Immunoblot analysis was performed using antibodies against PC1/3 and actin. Quantitative protein and transcripts levels are shown graphically. Results are displayed as means ± SEM. Indicated comparisons are significantly different: $^*P < 0.05$; $^{**}P < 0.01$; $^{***}P < 0.001$; n.s. indicates that no significant differences were observed between groups.

To confirm a β-cell–autonomous defect of SERCA2 deficiency, an SERCA2 knockout INS-1 832/13 cell line (S2KO) was generated. SERCA2b mRNA and SERCA2 protein were reduced in S2KO cells, but no significant alterations in *RyR2* or *IP3R3* expression were observed. *SERCA3* transcript levels were decreased by ∼40% in S2KO cells, but no reduction in SERCA3 protein level was observed (Fig. 7*D* and *E*). Consistent with the analysis performed in S2HET islets, expression of genes involved in ER stress signaling, including *Grp78*, *Dnajc3*, *Hsp90b1*, and *Pdia4* and the *spliced*-to-*total Xbp-1* ratio, were elevated in S2KO INS-1 cells under basal conditions and in response to GLT stress (Fig. 7*F*). Similar to results observed in islets from HFD-S2HET mice, immunoblot performed in S2KO cells also confirmed reduced levels of PC1/3 protein and mRNA (Fig. 7*G–I*).

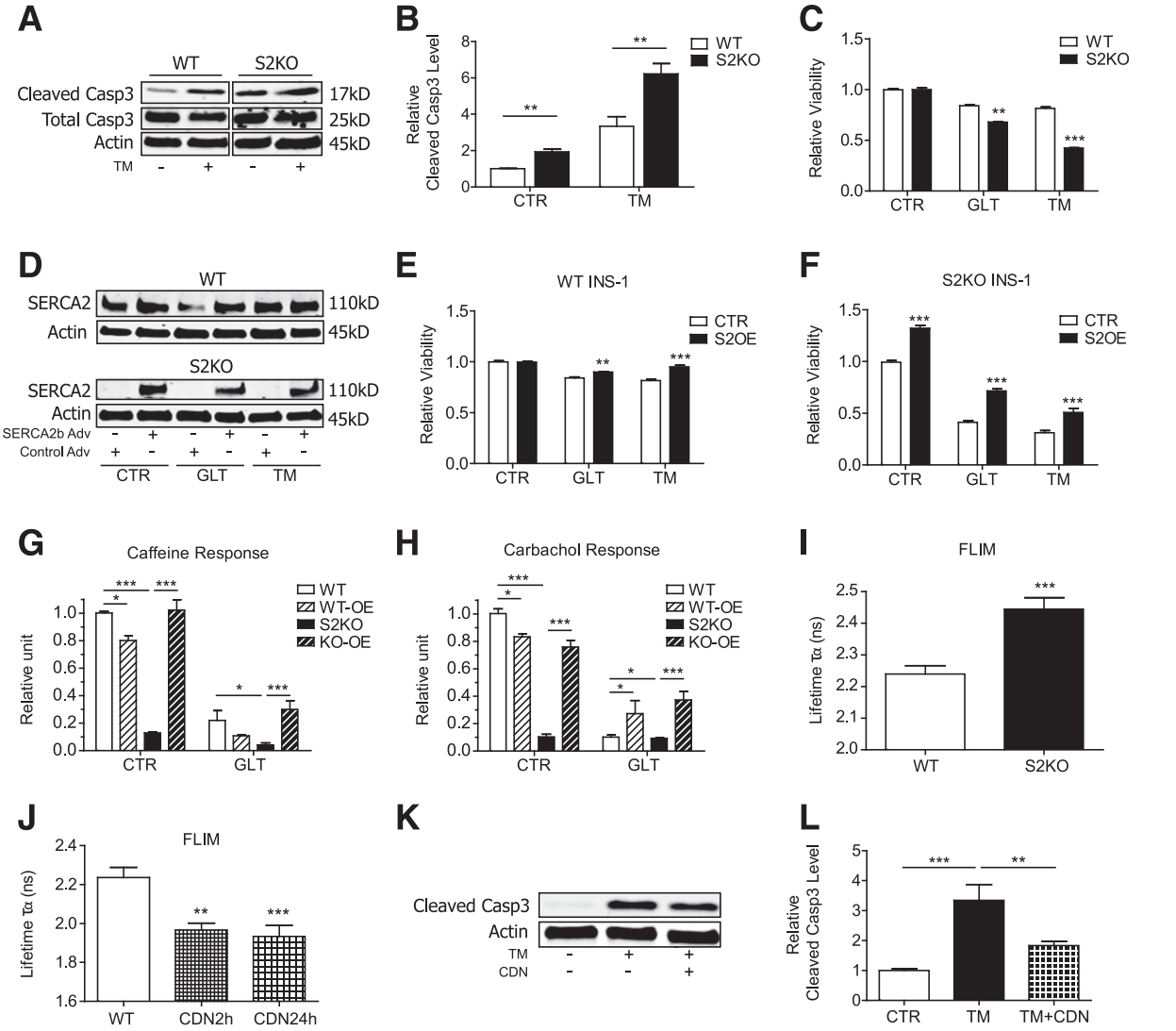

Figure 8—SERCA2 KO β-cells manifest impaired Ca^{2+} storage and increased susceptibility to stress-induced death. *A* and *B*: WT and S2KO INS-1 cells were treated with or without 10 μmol/L TM for 24 h. Immunoblot analysis was performed using antibodies against cleaved caspase-3 (Casp3), total caspase-3, and actin. Quantitative protein levels are shown graphically. *C*: WT and S2KO INS-1 cells were treated under control (CTR) conditions or exposed to GLT or TM for 24 h, and viability was measured using the CellTiter-Glo assay. Results were normalized to results obtained in WT cells under control conditions. *D–F*: SERCA2b was overexpressed (S2OE) via adenoviral (Adv) transduction in WT and S2KO INS-1 cells and then treated with GLT or TM for 24 h. *D*: Immunoblot analysis was performed using antibodies against SERCA2 and actin. CellTiter-Glo viability tests were performed in WT (*E*) and S2KO cells (*F*). Results were normalized to cells transduced with LacZ virus under control conditions. SERCA2b was overexpressed via adenoviral transduction in WT (WT-OE) and S2KO (KO-OE) INS-1 cells, followed by exposure to GLT for 24 h. *G* and *H*: To assess cytosolic Ca^{2+} levels, calcium 6 fluorescence was measured under Ca^{2+}-free conditions. *I* and *J*: INS-1 cells were transduced with a D4ER adenovirus, and FLIM was used to measure ER Ca^{2+}. Shown is the average donor lifetime in WT and S2KO INS-1 cells (*I*) or WT INS-1 cells treated with 10 μmol/L CDN1163 for 2 or 24 h (*J*) (n = at least 10 regions of interest per cell type or treatment). *K* and *L*: WT and S2KO INS-1 cells were treated with or without TM combined with or without 10 μmol/L CDN1163 for 24 h. Immunoblot analysis was performed using antibodies against cleaved caspase-3 and actin, and quantitative protein levels are shown graphically. Results are displayed as means ± SEM. Indicated comparisons were significantly different: $^*P < 0.05$; $^{**}P < 0.01$; $^{***}P < 0.001$.

SERCA2b Reconstitution Protects Against β-Cell Death and Ca^{2+} Dyshomeostasis in Response to ER and GLT Stress

S2KO and WT cells were next treated with tunicamycin (TM) to perturb protein folding through inhibition of protein glycosylation. Under control conditions and in response to TM, cleaved caspase-3 protein levels were significantly higher in S2KO cells (Fig. 8*A* and *B*). Similarly, S2KO cells exhibited decreased cell viability with TM- and GLT-induced stress (Fig. 8*C*). To test whether SERCA2 reconstitution was sufficient to reverse these effects, cells were transduced with an adenovirus expressing SERCA2b or LacZ (Fig. 8*D*). SERCA2b overexpression improved viability in both WT and S2KO cells treated with GLT and TM (Fig. 8*E* and *F*).

Ca^{2+} imaging experiments were next performed in S2KO and WT cells that had been treated with GLT or TM and transduced with the adenovirus expressing SERCA2b or LacZ. Carbachol and caffeine were used to stimulate IP3R- and RyR-mediated ER Ca^{2+} release, respectively, to provide an indirect assessment of ER Ca^{2+} storage (13). Results were analyzed as the change in Ca^{2+} (ΔF) in response to caffeine or carbachol, normalized to the baseline cytosolic Ca^{2+} level (F0). Under control conditions, S2KO cells exhibited a significant reduction in the ΔF-to-F0 ratio. The ΔF-to-F0 ratio was further decreased in GLT-treated WT and S2KO cells, whereas SERCA2b overexpression rescued the carbachol and caffeine response in S2KO cells and the carbachol response in WT cells (Fig. 8*G* and *H*). Similar to results obtained in S2HET islets, FLIM performed in S2KO cells also revealed a significant reduction in ER Ca^{2+} levels (Fig. 8*I*).

Finally, INS-1 cells were treated with the small molecule SERCA2 allosteric activator, CDN1163. Treatment with 10 μmol/L CDN1163 increased ER Ca^{2+} within 2 h, with no further increase observed after 24 h. Moreover, CDN1163 partially rescued TM-induced cleaved caspase-3 expression in WT INS-1 cells (Fig. 8*J–L*).

DISCUSSION

In rodent and human models of diabetes, acquired loss of SERCA2 expression and activity under inflammatory conditions has been correlated with altered β-cell Ca^{2+} homeostasis, reduced insulin secretion, and impaired β-cell survival, whereas SERCA2 restoration has been shown to improve these parameters (11,13). However, whether in vivo deficiency of SERCA2 is sufficient to impair systemic metabolic function and/or β-cell health has never been addressed. Homozygous loss of SERCA2 is embryonically lethal (23), so here mice with total-body SERCA2 heterozygosity (S2HET) were analyzed. Our results indicate that SERCA2 deficiency leads to impaired glucose tolerance and hyperglycemia in response to an HFD challenge. These alterations occurred secondary to decreased insulin production, altered β-cell Ca^{2+} homeostasis, decreased insulin secretion, reduced β-cell proliferation, and increased β-cell ER stress.

Similar to changes observed in the β-cell, several reports have revealed reduced SERCA2 expression in liver, skeletal muscle, and macrophages under diabetic conditions (24–28). Previous in vitro experiments have also shown that SERCA2 and SERCA1 interact with insulin receptor substrate 1 and 2 in skeletal muscle in an insulin-dependent manner, suggesting an effect of SERCA activity on glucose uptake (29). Furthermore, in vivo adenoviral-mediated restoration of SERCA2b expression in the liver improved glucose homeostasis in obese mice (24,28), whereas treatment with the SERCA activator CDN1163 improved hepatic ER stress and glucose tolerance in the *ob/ob* mouse model (30). In our study, however, S2HET and control mice exhibited indistinguishable patterns of weight gain, body composition, and systemic and tissue-specific insulin sensitivity, suggesting that the glucose intolerance observed in the HFD-fed S2HET mice did not arise from perturbations in adiposity or insulin sensitivity. Rather, we conclude the phenotype of this model was largely driven by an impaired β-cell compensatory response to diet-induced obesity.

The ER is a key intracellular Ca^{2+} store, wherein the intraluminal Ca^{2+} concentration is estimated to be at least several orders of magnitude higher than cytosolic Ca^{2+}. The SERCA family of ATPases is the only known group of transporters tasked with Ca^{2+} uptake into the ER lumen, whereas ER Ca^{2+} release occurs via the RyRs and IP3Rs, which become activated in response to specific ligands or intracellular signaling pathways (31,32). To date, the in vivo role of the IP3R in the pancreatic β-cell has yet to be studied. However, a single-point mutation in the RyR, leading to unregulated ER Ca^{2+} leak, resulted in decreased insulin secretion, impaired glucose tolerance, increased β-cell ER stress, and mitochondrial dysfunction (33). These results as well as our study emphasize a pivotal role for ER Ca^{2+} homeostasis in the maintenance of β-cell function and health.

Three different SERCA genes (*ATP2A1*, *ATP2A2*, and *ATP2A3*) encode the proteins SERCA1, -2, and -3, and at least 14 isoforms are expressed as a result of alternative splicing. Temporal patterns of isoform expression during development and tissue-specific patterns of expression postnatally suggest nonredundant function of individual isoforms (10). Three isoforms, SERCA2a, -2b, and -3, are expressed in the β-cell. SERCA2b is the most highly expressed, and SERCA3 mRNA is expressed at ~50% of the level of SERCA2b in mouse islets. SERCA2a is expressed at a level of ~1% that of SERCA2b (11). This distinction is important because our mouse and cell line model included loss of both SERCA2a and -2b. However, given the low levels of SERCA2a expression, the role of this isoform in the β-cell is unclear. Moreover, our results suggest that overexpression of just SERCA2b in S2KO INS-1 cells is sufficient to rescue Ca^{2+} homeostasis and TM- and GLT-induced cell death. Structurally, SERCA2b is unique among all of the other isoforms because it contains an extra 11th transmembrane helix with an associated ER luminal extension or "2b tail" imparting this isoform with the highest Ca^{2+} affinity (34).

SERCA3 function in the islet was previously investigated in series of elegant studies by Gilon and colleagues (9,35) using mice with homozygous and whole-body SERCA3 deletion. Under chow-fed conditions, SERCA3 KO mice exhibited normal glucose tolerance without overt evidence of ER stress. SERCA3 ablation also did not affect basal cytosolic Ca^{2+} levels or the initial glucose-induced Ca^{2+} response within islets (35). After glucose stimulation, SERCA3-null islets exhibited a higher phase 2 cytosolic Ca^{2+} oscillatory amplitude, consistent with impaired ER Ca^{2+} uptake that interestingly led to increased insulin secretion (9).

Although SERCA3 mice have never been challenged with diet-induced obesity, somewhat limiting direct comparisons, our results still suggest nonoverlapping function for the two isoforms. We show that SERCA2 haploinsufficiency, combined with HFD stress, led to increased basal cytosolic Ca^{2+} levels, impaired glucose and KCl-stimulated Ca^{2+} responses, and delayed onset of glucose-induced Ca^{2+} oscillations. In aggregate, these results suggest a broader role for SERCA2 in patterning β-cell Ca^{2+} architecture and insulin secretion that is independent of glucose sensing and ATP generation. In contrast to SERCA3-null islets, perturbations in Ca^{2+} signaling in SERCA2-deficient islets were sufficient to impair GSIS both in vivo and ex vivo. Notably, no compensatory upregulation of SERCA3 protein expression in our mouse model or in the clonal SERCA2 KO β-cell line was observed.

In addition to altering insulin secretion, SERCA2 deficiency also had a significant effect on β-cell ER health. S2HET islets exhibited altered ER morphology and increased expression of genes involved in ER stress signaling, whereas SERCA2-deficient INS-1 cells were more susceptible to GLT- and TM-induced cell death. Previous work has shown that β-cell ER stress results in insulin mRNA degradation through hyperactivation of inositol-requiring enzyme 1α, whereas protein kinase RNA-like ER kinase activation suppressed insulin translation (36–38). Consistent with these studies, islet insulin mRNA and protein levels were decreased, and circulating insulin levels were lower in HFD-fed S2HET mice compared with age- and diet-matched WT controls. In addition to defective insulin production, S2HET islets also exhibited impaired insulin processing and decreased insulin granule maturation after HFD.

Proteolytic cleavage of proinsulin into mature insulin requires activity of PC1/3, PC2, and carboxypeptidase E within secretory granules. Ca^{2+} is also required to direct PC1/3 into dense core secretory granules (39) while further serving as an essential cofactor for both PC1/3 and 2 activity (8). The Ca^{2+} content within secretory granules is patterned by ER Ca^{2+} levels, suggesting a relationship between SERCA2 deficiency and convertase enzyme activity (40). An unanticipated finding in our study was that PC1/3 mRNA and protein expression were also decreased in S2HET islets and S2KO cells. Regarding this point, a recent study in GLUTag murine enteroendocrine cells, which secrete glucagon-like peptide, also revealed decreased PC1/3 protein levels with palmitate-induced ER stress (41). A similar effect was observed in MIN-6 β-cells after 7 days of palmitate and oleate treatment (42).

Finally, our data also show that SERCA2 deficiency resulted in decreased β-cell proliferation in response to diet-induced obesity. A number of important Ca^{2+}-regulated proliferative pathways have been identified in the β-cell, including those regulated by nuclear factor of activated T-cells (NFAT) and cAMP-response element–binding protein (CREB), which are both activated in response to a rise in cytosolic Ca^{2+} (43–45). Moreover, a direct relationship between ER stress and β-cell proliferation has also been suggested by two recent studies. Sharma et al. (46) showed that mild ER stress favored β-cell proliferation, whereas Szabat et al. (47) showed that reduced insulin production relieved β-cell ER stress and induced β-cell proliferation. Precisely how altered SERCA2 activity in our model affects known Ca^{2+}-dependent proliferative pathways and integrates with the above studies will be the subject of future investigation.

In summary, we provide evidence that loss of SERCA2 leads to a cell-autonomous defect in β-cell secretory function, Ca^{2+} homeostasis, proliferation, and survival. Although tissue-specific deletion models are needed to fully resolve the effects of SERCA2 loss on β-cell function and peripheral insulin sensitivity, our data and those of others suggest that strategies aimed at restoration of SERCA2 expression and/or modulation of SERCA2 activity represent viable strategies to improve glucose homeostasis (24,28,30). Finally, these data also have relevance for humans with Darier-White disease, in which one copy of the *ATP2A2* gene is defective. Although the metabolic effects of SERCA2 haploinsufficiency have not been reported in these individuals, a selective predisposition to diet-induced metabolic disease and other conditions, such as heart disease (48), could easily be overlooked in this rare population and should be further studied.

Acknowledgments. The authors acknowledge the support of the Islet and Physiology, Translation, and Imaging Cores of the Indiana Diabetes Research Center (P30-DK-097512).

Funding. X.T. was supported by the Diabetes and Obesity DeVault Fellowship at the Indiana University School of Medicine. This work was supported by National Institute of Diabetes and Digestive and Kidney Diseases grants R01-DK-093954 and UC4-DK-104166 (to C.E.-M.), U.S. Department of Veterans Affairs Merit Award I01BX001733 (to C.E.-M.), and gifts from the Sigma Beta Sorority, the Ball Brothers Foundation, and the George and Frances Ball Foundation (to C.E.-M.).

Duality of Interest. No potential conflicts of interest relevant to this article were reported.

Author Contributions. X.T. contributed to study conception and design, data acquisition and analysis and interpretation and drafted the article. T.K. contributed to study conception and design, data acquisition, and review of the manuscript. E.K.A.-B. contributed to data acquisition and critical revision of the manuscript. W.Y. contributed to data acquisition. P.G. and D.L. contributed critical reagents, contributed to data analysis, and provided critical revision of the

manuscript. R.N.D. contributed to data acquisition and analysis and critical revision of the manuscript. G.E.S. kindly provided the SERCA2 heterozygous mouse model and provided critical revision of the manuscript. C.E.-M. contributed to study conception and design, data analysis and interpretation, critical revision of the manuscript, and final approval of the manuscript. All authors approved the manuscript. C.E.-M. is the guarantor of this work, and, as such, had full access to all the data in the study and takes responsibility for the integrity of the data and the accuracy of the data analysis.

Prior Presentation. Parts of this study were presented at the 75th Scientific Sessions of the American Diabetes Association, Boston, MA, 5–9 June 2015, and at the Experimental Biology 2016 Meeting, San Diego, CA, 2–6 April 2016.

References

1. International Diabetes Federation. *IDF Diabetes Atlas, 7th edition*. Brussels Belgium, International Diabetes Federation, 2015. Available from http://www.diabetesatlas.org. Accessed 15 March 2016
2. Holman RR, Paul SK, Bethel MA, Matthews DR, Neil HA. 10-year follow-up of intensive glucose control in type 2 diabetes. N Engl J Med 2008;359:1577–1589
3. Butler AE, Janson J, Bonner-Weir S, Ritzel R, Rizza RA, Butler PC. β-cell deficit and increased β-cell apoptosis in humans with type 2 diabetes. Diabetes 2003;52:102–110
4. Bygrave FL, Benedetti A. What is the concentration of calcium ions in the endoplasmic reticulum? Cell Calcium 1996;19:547–551
5. Varadi A, Rutter GA. Dynamic imaging of endoplasmic reticulum Ca2+ concentration in insulin-secreting MIN6 cells using recombinant targeted cameleons: roles of sarco(endo)plasmic reticulum Ca2+-ATPase (SERCA)-2 and ryanodine receptors. Diabetes 2002;51(Suppl. 1):S190–S201
6. Lytton J, Westlin M, Burk SE, Shull GE, MacLennan DH. Functional comparisons between isoforms of the sarcoplasmic or endoplasmic reticulum family of calcium pumps. J Biol Chem 1992;267:14483–14489
7. Chen L, Koh DS, Hille B. Dynamics of calcium clearance in mouse pancreatic β-cells. Diabetes 2003;52:1723–1731
8. Guest PC, Bailyes EM, Hutton JC. Endoplasmic reticulum Ca2+ is important for the proteolytic processing and intracellular transport of proinsulin in the pancreatic beta-cell. Biochem J 1997;323:445–450
9. Ravier MA, Daro D, Roma LP, et al. Mechanisms of control of the free Ca2+ concentration in the endoplasmic reticulum of mouse pancreatic β-cells: interplay with cell metabolism and [Ca2+]c and role of SERCA2b and SERCA3. Diabetes 2011;60:2533–2545
10. Periasamy M, Kalyanasundaram A. SERCA pump isoforms: their role in calcium transport and disease. Muscle Nerve 2007;35:430–442
11. Kono T, Ahn G, Moss DR, et al. PPAR-γ activation restores pancreatic islet SERCA2 levels and prevents β-cell dysfunction under conditions of hyperglycemic and cytokine stress. Mol Endocrinol 2012;26:257–271
12. Johnson JS, Kono T, Tong X, et al. Pancreatic and duodenal homeobox protein 1 (Pdx-1) maintains endoplasmic reticulum calcium levels through transcriptional regulation of sarco-endoplasmic reticulum calcium ATPase 2b (SERCA2b) in the islet β cell. J Biol Chem 2014;289:32798–32810
13. Tong X, Kono T, Evans-Molina C. Nitric oxide stress and activation of AMP-activated protein kinase impair β-cell sarcoendoplasmic reticulum calcium ATPase 2b activity and protein stability. Cell Death Dis 2015;6:e1790
14. Alessandra K, Cardozo FO, Storling J, et al. Cytokines downregulate the sarcoendoplasmic reticulum pump Ca ATPase 2b and deplete endoplasmic reticulum Ca, leading to induction of endoplasmic reticulum stress in pancreatic beta-cells. Diabetes 2005;54:452–461
15. Sakuntabhai A, Ruiz-Perez V, Carter S, et al. Mutations in ATP2A2, encoding a Ca2+ pump, cause Darier disease. Nat Genet 1999;21:271–277
16. Fisher MM, Perez Chumbiauca CN, Mather KJ, Mirmira RG, Tersey SA. Detection of islet β-cell death in vivo by multiplex PCR analysis of differentially methylated DNA. Endocrinology 2013;154:3476–3481
17. Sims EK, Hatanaka M, Morris DL, et al. Divergent compensatory responses to high-fat diet between C57BL6/J and C57BLKS/J inbred mouse strains. Am J Physiol Endocrinol Metab 2013;305:E1495–E1511
18. Stull ND, Breite A, McCarthy R, Tersey SA, Mirmira RG. Mouse islet of Langerhans isolation using a combination of purified collagenase and neutral protease. J Vis Exp 2012:4137
19. Wijesekara N, Dai FF, Hardy AB, et al. Beta cell-specific Znt8 deletion in mice causes marked defects in insulin processing, crystallisation and secretion. Diabetologia 2010;53:1656–1668
20. Hatanaka M, Maier B, Sims EK, et al. Palmitate induces mRNA translation and increases ER protein load in islet β-cells via activation of the mammalian target of rapamycin pathway. Diabetes 2014;63:3404–3415
21. Evans-Molina C, Robbins RD, Kono T, et al. Peroxisome proliferator-activated receptor gamma activation restores islet function in diabetic mice through reduction of endoplasmic reticulum stress and maintenance of euchromatin structure. Mol Cell Biol 2009;29:2053–2067
22. Alarcon C, Boland BB, Uchizono Y, et al. Pancreatic β-cell adaptive plasticity in obesity increases insulin production but adversely affects secretory function. Diabetes 2016;65:438–450
23. Periasamy M, Reed TD, Liu LH, et al. Impaired cardiac performance in heterozygous mice with a null mutation in the sarco(endo)plasmic reticulum Ca2+-ATPase isoform 2 (SERCA2) gene. J Biol Chem 1999;274:2556–2562
24. Fu S, Yang L, Li P, et al. Aberrant lipid metabolism disrupts calcium homeostasis causing liver endoplasmic reticulum stress in obesity. Nature 2011;473:528–531
25. Rácz G, Szabó A, Vér A, Zádor E. The slow sarco/endoplasmic reticulum Ca2+ -ATPase declines independently of slow myosin in soleus muscle of diabetic rats. Acta Biochim Pol 2009;56:487–493
26. Bayley JS, Pedersen TH, Nielsen OB. Skeletal muscle dysfunction in the db/db mouse model of type 2 diabetes. Muscle Nerve 2016;54:460–468
27. Liang CP, Han S, Li G, Tabas I, Tall AR. Impaired MEK signaling and SERCA expression promote ER stress and apoptosis in insulin-resistant macrophages and are reversed by exenatide treatment. Diabetes 2012;61:2609–2620
28. Park SW, Zhou Y, Lee J, Lee J, Ozcan U. Sarco(endo)plasmic reticulum Ca2+-ATPase 2b is a major regulator of endoplasmic reticulum stress and glucose homeostasis in obesity. Proc Natl Acad Sci U S A 2010;107:19320–19325
29. Algenstaedt P, Antonetti DA, Yaffe MB, Kahn CR. Insulin receptor substrate proteins create a link between the tyrosine phosphorylation cascade and the Ca2+-ATPases in muscle and heart. J Biol Chem 1997;272:23696–23702
30. Kang S, Dahl R, Hsieh W, et al. Small molecular allosteric activator of the sarco/endoplasmic reticulum Ca2+-ATPase (SERCA) attenuates diabetes and metabolic disorders. J Biol Chem 2016;291:5185–5198
31. Islam MS, Leibiger I, Leibiger B, et al. In situ activation of the type 2 ryanodine receptor in pancreatic beta cells requires cAMP-dependent phosphorylation. Proc Natl Acad Sci U S A 1998;95:6145–6150
32. Bootman MD, Berridge MJ. The elemental principles of calcium signaling. Cell 1995;83:675–678
33. Santulli G, Pagano G, Sardu C, et al. Calcium release channel RyR2 regulates insulin release and glucose homeostasis. J Clin Invest 2015;125:1968–1978
34. Vandecaetsbeek I, Trekels M, De Maeyer M, et al. Structural basis for the high Ca2+ affinity of the ubiquitous SERCA2b Ca2+ pump. Proc Natl Acad Sci U S A 2009;106:18533–18538
35. Arredouani A, Guiot Y, Jonas JC, et al. SERCA3 ablation does not impair insulin secretion but suggests distinct roles of different sarcoendoplasmic reticulum Ca(2+) pumps for Ca(2+) homeostasis in pancreatic beta-cells. Diabetes 2002;51:3245–3253
36. Lipson KL, Ghosh R, Urano F. The role of IRE1α in the degradation of insulin mRNA in pancreatic β-cells. PLoS One 2008;3:e1648
37. Pirot P, Naamane N, Libert F, et al. Global profiling of genes modified by endoplasmic reticulum stress in pancreatic beta cells reveals the early degradation of insulin mRNAs. Diabetologia 2007;50:1006–1014
38. Ron D. Translational control in the endoplasmic reticulum stress response. J Clin Invest 2002;110:1383–1388
39. Dikeakos JD, Di Lello P, Lacombe MJ, et al. Functional and structural characterization of a dense core secretory granule sorting domain from the PC1/3 protease. Proc Natl Acad Sci U S A 2009;106:7408–7413

40. Petersen OH. Ca^{2+} signalling in the endoplasmic reticulum/secretory granule microdomain. Cell Calcium 2015;58:397–404
41. Hayashi H, Yamada R, Das SS, et al. Glucagon-like peptide-1 production in the GLUTag cell line is impaired by free fatty acids via endoplasmic reticulum stress. Metabolism 2014;63:800–811
42. Furukawa H, Carroll RJ, Swift HH, Steiner DF. Long-term elevation of free fatty acids leads to delayed processing of proinsulin and prohormone convertases 2 and 3 in the pancreatic beta-cell line MIN6. Diabetes 1999;48:1395–1401
43. Jhala US, Canettieri G, Screaton RA, et al. cAMP promotes pancreatic beta-cell survival via CREB-mediated induction of IRS2. Genes Dev 2003;17:1575–1580
44. Heit JJ, Apelqvist AA, Gu X, et al. Calcineurin/NFAT signalling regulates pancreatic beta-cell growth and function. Nature 2006;443:345–349
45. Hussain MA, Porras DL, Rowe MH, et al. Increased pancreatic β-cell proliferation mediated by CREB binding protein gene activation. Mol Cell Biol 2006; 26:7747–7759
46. Sharma RB, O'Donnell AC, Stamateris RE, et al. Insulin demand regulates β cell number via the unfolded protein response. J Clin Invest 2015;125: 3831–3846
47. Szabat M, Page MM, Panzhinskiy E, et al. Reduced insulin production relieves endoplasmic reticulum stress and induces β cell proliferation. Cell Metab 2016;23:179–193
48. Prasad V, Lorenz JN, Lasko VM, et al. SERCA2 haploinsufficiency in a mouse model of Darier disease causes a selective predisposition to heart failure. BioMed Res Int 2015;2015:251598